Drug Design, Development and Therapy

Dovepress
open access to scientific and medical research

Open Access Full Text Article

ORIGINAL RESEARCH

Applications of daunorubicin-loaded PLGA-PLL-PEG-Tf nanoparticles in hematologic malignancies: an in vitro and in vivo evaluation

This article was published in the following Dove Medical Press journal:
Drug Design, Development and Therapy

Wen Bao
Ran Liu
Guohua Xia
Fei Wang
Baoan Chen

Department of Hematology and Oncology, Key Medical Disciplines of Jiangsu Province, Zhongda Hospital, Medical School of Southeast University, Nanjing 210009, People's Republic of China

Background: With the development of drug delivery, novel tools and technological approaches have captured the attention of researchers in recent years. Several target drug delivery systems (DDSs) including nanoparticles (NPs) have been developed as an important strategy to deliver classical medicine.

Objective: The objective of this study was to evaluate the application of novel daunorubicin (DNR)-loaded poly(lactic-co-glycolic acid)-poly-L-lysine-polyethylene glycol-transferrin (Tf) nanoparticles (DNR-loaded NPs) in hematologic malignancies in vitro and in vivo.

Materials and methods: DNR-loaded NPs were prepared by the modified double-emulsion solvent evaporation/diffusion method, and its microscopic form was observed under scanning electron microscope. Intracellular distribution of DNR was directly detected by fluorescence microscopy. After establishment of a tumor xenograft model by injecting K562 cells into the left leg of nude mice, the therapeutic effect of the DNR-loaded NPs on the growth of tumors was measured by calculating the tumor size, and the relative expression of Caspase-3 protein was detected by immunohistochemical staining. Furthermore, intracellular concentration of DNR and the extent of cell apoptosis in primary leukemia cells were quantified by flow cytometry.

Results: DNR-loaded NPs had a spherical shape of about 180 nm in diameter. DNR-loaded NP group showed a significant enhancement of cellular uptake in K562 cells compared with DNR group. Tumor inhibition rate was higher in DNR-loaded NP group in comparison with DNR group, and the relative expression of Caspase-3 protein was upregulated in DNR-loaded NP group compared with DNR group. Furthermore, DNR-loaded NPs obviously increased intracellular concentration of DNR in primary leukemia cells compared with DNR group, but there was no significant difference in primary cell apoptosis between the two groups. These findings suggest that the novel NP DDS can enhance the performance of conventional antitumor drugs and may be suitable for further application in the treatment of hematologic malignancies.

Keywords: nanoparticles, transferrin, targeted drug delivery system, leukemia

Introduction

Cancer is a serious public health problem since it has become a leading cause of death. Current chemotherapeutic agents are mostly non-selective; even a regular dose will cause significant side effects to normal tissues and organs, and patients usually cannot tolerate them for long periods of time. As a result, drug delivery methods for specific delivery of drugs to tumor cells, increasing drug intake of tumor cell and reducing the dosage of treatment, are crucial for cancer treatment. In the early 1900s, Ehrlich was the first to develop the concept of targeted drug delivery system (DDS), which has been widely studied in the subsequent decades. Targeted therapy is based

Correspondence: Baoan Chen
Department of Hematology and Oncology, Key Medical Disciplines of Jiangsu Province, Zhongda Hospital, Medical School of Southeast University, DingJiaQiao 87, Nanjing 210009, People's Republic of China
Email cba8888@hotmail.com

submit your manuscript | www.dovepress.com
Dovepress
http://dx.doi.org/10.2147/DDDT.S195832

on either passive or active processes, in which passive targeting depends on the physical properties and the size of the delivery system to target the tumor microenvironment, whereas active targeting relies on a specific receptor on the tumor cell as surface targeting moieties.[1]

It is well known that the transferrin receptor (TfR) is highly expressed in fast growing tumor cells[2,3] and that the expression of TfR is negatively correlated with tumor staging and prognosis.[4–6] Accumulating evidence has demonstrated that the expression of TfR in some tumors is more than 100 times higher than that in normal cells.[7,8] Thus, targeted chemotherapy using transferrin and TfR as the targeting moiety is shown to be important to cancer-specific therapies. In fact, targeted chemotherapeutic agents can enhance cellular uptake via Tf-mediated mechanisms and increase selective cytotoxicity in cancer cell lines.[1]

Nanoparticles (NPs), with diameters ranging from 1 to 1,000 nm, have been developed in DDS. Interestingly, therapeutic agents are encapsulated within or bound to biocompatible nanocarriers to form a nanosphere or nanocapsule.[9] As an ideal NP DDS, it could reach the tumor cell via a molecular-targeted delivery, where it would release anticancer agents into the tumor cell directly.[10]

In this study, we synthesized a new type of nanoparticulate system that was composed of biocompatible and biodegradable polymers, polyethylene glycol (PEG), poly-L-lysine (PLL), and poly(lactic-*co*-glycolic acid) (PLGA), the surface of which was modified with transferrin. PLGA-PLL-PEG-Tf NPs enhanced cellular uptake in cancer cells and increased the sensitivity of anticancer drugs in vivo, suggesting that PLGA-PLL-PEG-Tf NPs may be a complete DDS for the clinical therapy of hematologic malignancies.

Materials and methods

Main reagent and culture medium

Daunorubicin (DNR) was purchased from Main Luck Pharmaceuticals Inc (Shenzhen, China), Roswell Park Memorial Institute(RPMI)-1640 from Thermo Fisher Scientific (Waltham, MA, USA), FBS, and DAPI from Sigma-Aldrich Co. (St Louis, MO, USA), UltraSensitiveTM S-P IHC Kit from Nanjing KeyGen Biotech Co. Ltd. (Nanjing, China). PLGA-PLL-PEG-Tf-NPs and DNR-PLGA-PLL-PEG-Tf-NPs were synthesized according to our previously reported study[11,12] and purified by College of Pharmacy, Nanjing University of Technology (Nanjin, China).

Cell line, primary cell, and animals

Leukemia K562 cells were obtained from Institute of Hematology, Chinese Academy of Medical Sciences (Beijing, China), and primary leukemia cells were obtained from the Department of Hematology of Zhongda Hospital (Nanjin, China). The patients involved in the present study provided written informed consent, and the Institutional Review Board of Zhongda Hospital, Medical School of Southeast University approved the study. BALB/c nude mice at 7 weeks of age were obtained from Shanghai National Center for Laboratory Animals (Shanghai, China). Animal care, surgical procedures, and experimental protocols were approved by the Medical Ethics Committee on the Care and Use of Laboratory Animals of Southeast University (the approval number is 20171110004).

Scanning electron microscopy (SEM) to observe the microscopic form of drug-loaded NPs

DNR-loaded NPs were fixed on the sample table. Then, gold was plated on the surface of DNR-loaded NPs, and then the samples were observed and photographed under SEM (Hitachi Ltd, Tokyo, Japan).

Cell culture and evaluating intracellular drug concentration

K562 cells were grown in RPMI-1640 medium including 10% inactivated fetal calf serum, 100 U/mL penicillin, and 100 μg/mL streptomycin in a humidified 37°C, 5% CO_2-air incubator and passaged every 2 or 3 days. The logarithmic phase of K562 cells at a concentration of 1.0×10^4 cells/well were exposed to the medium (control group), DNR (DNR group), PLGA-PLL-PEG-Tf nanoparticles (NP group), and DNR-PLGA-PLL-PEG-Tf NPs with equivalent concentration of DNR (DNR-loaded NP group) for 12 hours. Then the cells were collected and washed three times with PBS. Thereafter, the cells were stained with DAPI for 15 minutes in the dark, and the drug distribution of the cells was observed at least 100 cells per sample in different fields of view under fluorescence microscopy (400×, IX51; Olympus Corporation, Tokyo, Japan).

Establishing xenograft tumor model of nude mice and detecting therapeutic effect of drug in them

K562 cells at the concentration of 1×10^7/0.2 mL were subcutaneously inoculated into the left leg of each nude mouse. Once palpable tumors were detected and the average tumor volume reached 50 mm^3, tumor-burdened mice were randomly divided into four groups of six animals each: control group, NP group, DNR group, and DNR-loaded NP group, in which the single dosage of DNR was 1 mg/kg and the dosage of DNR-loaded NPs contained 1 mg/kg DNR

for the single injection. The experimental treatments were done once every other day for nine times. During the whole study period, symptoms of toxicity were monitored, and the size of tumors was measured with a digital caliper and the tumor volume (V/mm^3) was calculated according to the formula $V = 1/2 (a \times b^2)$, where a is the longest diameter and b is the shortest one. The relative tumor volume (RTV) was calculated according to the formula $RTV = V_X/V_0$, where V_X and V_0 represent the volume on day X and the first day before treatment, respectively, and tumor inhibition rate is defined as the inhibitory rate (IR) = $(1 - RTV_{experimental\ group}/RTV_{control\ group})$. All studies were performed in adherence with the Guidelines for the Care and Use of Laboratory Animals established by the National Institute of Health.

Immunohistochemical staining

After deparaffinization and rehydration, immunohistochemical staining of paraffin-embedded tumor tissue sections was performed using UltraSensitiveTM S-P IHC Kit according to the manufacturer's protocols. Briefly, the sections were incubated with anti-Caspase 3 antibody (1:100; Boster Biological Technology, Ltd., Wuhan, China) at 4°C overnight and reincubated with biotinylated goat-anti-rabbit IgG (1:100; Boster Biological Technology, Ltd.) for 30 minutes. After washing in PBS three times for 5 minutes, the signal was visualized using 0.05% diaminobenzidine substrate and counterstained with hematoxylin. Thereafter, the sections were examined and microphotographed under an Olympus IX51 microscope (400×; Olympus Corporation). Brown cytoplasmic staining was considered to be positive for Caspase 3, and the relative optical density of Caspase 3 was calculated as integral optical density $(IOD)_{treated\ group}/IOD_{control\ group}$ by using Image-pro plus 6.0 (Media Cybernetics, Silver Spring, MD, USA).

Primary leukemia cell culture

Primary leukemia cells were collected from an untreated adult male patient with acute leukemia. Briefly, 3 mL peripheral blood (immature cells >70%) of the patient was collected and kept in a heparin anticoagulant tube. Then the primary leukemia cells were isolated by Ficoll-Hypaque gradient centrifugation and grown in RPMI-1640 medium supplemented with 20% of FBS, placed in 37°C, 5% CO_2 humidified incubator. The cells used in the experiments were in logarithmic growth phase.

Intracellular concentration of DNR in the primary leukemia cells

The primary leukemia cells (2×10^6) seeded in six-well plates were exposed to the medium, NPs, DNR, and DNR-loaded NPs. After incubation for 48 hours, the cells were collected and washed three times with PBS. Then, intracellular accumulation of DNR was detected by FACSCalibur flow cytometry (FCM; BD Diagnostics, Franklin Lakes, NJ, USA) at the excitation wavelength of 488/575 nm, and the relative fluorescence intensity (RFI) was calculated as $FI_{treated\ cells}/FI_{control\ cells}$.

Apoptosis of primary leukemia cells determined by FCM

The primary leukemia cells were incubated and collected by the above methods. Then the washed cells were suspended with 500 μL binding buffer and labeled with 5 μL Annexin V-FITC for 15 minutes at room temperature in the dark. Thereafter, cell apoptosis was determined by FACSCalibur FCM (BD Diagnostics).

Statistical analysis

Data were expressed as mean ± SD from triplicate experiments and analyzed by SPSS software (version 13.0; SPSS Inc, Chicago, IL, USA). The difference of statistical significance was determined by one-way analysis of variance among multiple groups, and differences with $P<0.05$ were considered statistically significant.

Results

Size and image of DNR-PLGA-PLL-PEG-Tf NPs under SEM

The surface morphology of DNR-PLGA-PLL-PEG-Tf NPs under SEM was smooth. Most of the NPs were spherical in shape or approximately spherical surfaces, and the diameter of NPs was about 180 nm (Figure 1).

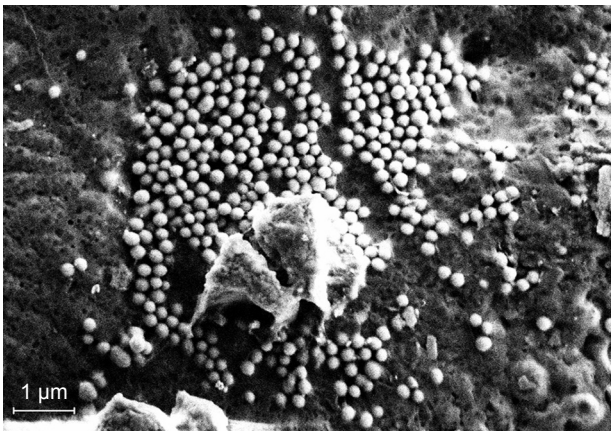

Figure 1 Representative image of DNR-PLGA-PLL-PEG-Tf-nanoparticles under SEM (bar =1 μm in the field).
Abbreviations: DNR-PLGA-PLL-PEG-Tf, daunorubicin-loaded poly(lactic-co-glycolic acid)-poly-L-lysine-polyethylene glycol-transferrin; SEM, scanning electron microscopy.

Intracellular distribution of DNR in K562 cells

Owing to spontaneous emission of red fluorescence, intracellular distribution of DNR was directly detected by fluorescence microscopy (Figure 2). After dyeing, the DAPI-stained nuclei in blue fluorescence in K562 cells were used for cellular localization, in which the red fluorescence emitting from DNR can be observed in both DNR group and DNR-loaded NP group, whereas no red fluorescence was observed in both control group and NP group. Notably, the red fluorescence intensity was obviously stronger and the level of red fluorescence was more in the DNR-loaded NP group compared with DNR group, suggesting that intracellular DNR concentration in DNR-loaded NP group was higher than DNR group and that PLGA-PLL-PEG-Tf NPs enhance the intake of DNR in K652 cells.

Toxicity, tumor volume, and relative tumor inhibitory rate

There were no obvious symptoms of toxicity observed in animals during treatment, and the tumor inhibition rate was 78.43%±3.92% in the DNR-loaded NP group and 51.23%±4.51% in the DNR group, both of them are higher than the NP group (5.91%±2.30%) (all $P<0.05$). Whereas, there was no obvious difference of inhibitory rate between control group and PLGA-PLL-PEG-Tf-NP group ($P>0.05$). Notably, the tumor inhibitory rate was higher in the DNR-loaded NP group than that in the DNR group ($P<0.05$; Figure 3). These results suggest that DNR-loaded NPs have the strongest effect on tumor inhibitory rate in K562 xenografts.

Apoptosis-related protein detected by immunohistochemical staining

After treatment for 18 days, the tumor tissues obtained from the mouse models were used for further immunohistochemical studies on Caspase 3 distribution. As shown in Figure 4, the relative optical density of Caspase 3 in both DNR group and DNR-loaded NP group was upregulated compared with that in the control group (all $P<0.05$), and the increase was more dramatic in the DNR-loaded NP group compared with DNR group ($P<0.05$; Figure 4E). But there was no significant difference of the relative optical density of Caspase 3 between the control group and NP group ($P>0.05$). These data indicate that the targeted NP DDS substantially enhanced the antitumor activity of traditional chemotherapeutic agents.

Concentration of DNR in the acute primary leukemia cells

After incubated for 48 hours, RFI of DNR in the DNR group and DNR-loaded NP group was 3.11±0.12 and 4.17±0.19, respectively (Figure 5A–D). Compared with the control

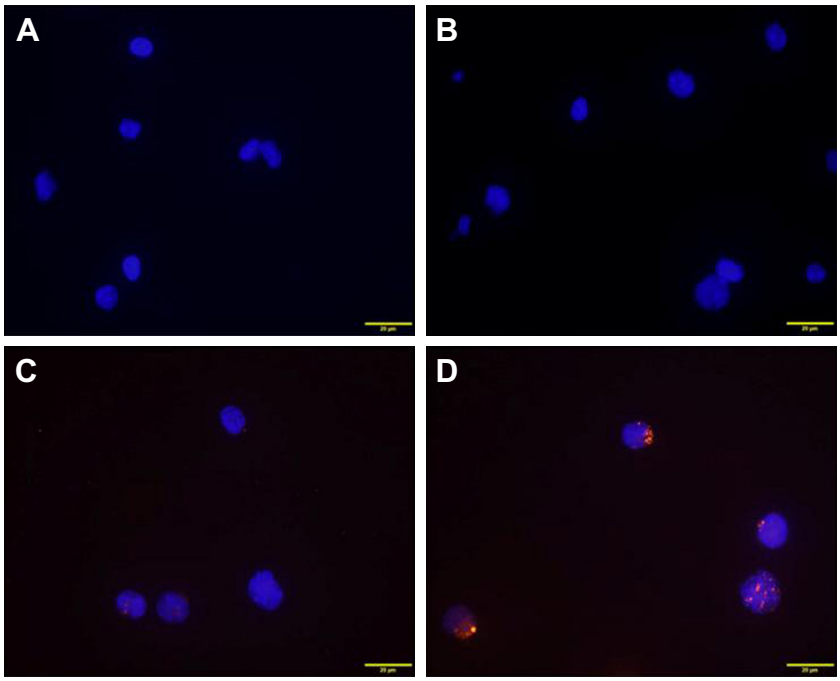

Figure 2 Intracellular distribution of DNR in leukemia K562 cells in control (**A**), NP (**B**), DNR (**C**), and DNR-loaded NP (**D**) groups under fluorescence microscopy (×400).
Abbreviations: DNR, daunorubicin; NP, nanoparticle.

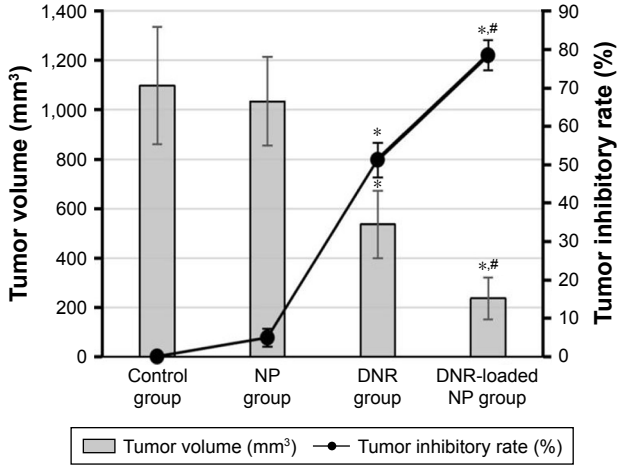

Figure 3 Relative tumor inhibitory rate of mice after treatment for 18 days. Data expressed as mean ± SD (n=6). *$P<0.05$ when compared with the control group, #$P<0.05$ when compared with the DNR group.
Abbreviations: DNR, daunorubicin; NP, nanoparticle.

group, intracellular DNR accumulation increased in both DNR and DNR-loaded NPs ($P<0.05$). Notably, intracellular DNR concentration of DNR-loaded NP group was higher compared with DNR group ($P<0.05$; Figure 5E).

Determination of cell apoptosis in acute primary leukemia cells

After incubated for 48 hours, the apoptosis rate of acute primary leukemia cells was detected. The result showed that apoptosis rate of the cells in control group was 18.24%±2.20% and that in NP group was 19.05%±3.50%, DNR group was 83.96%±6.96%, and DNR-loaded NP group was 90.72%±6.81%. Compared with the control group, both DNR and DNR-loaded NPs significantly increased the apoptosis rate ($P<0.05$), whereas the apoptosis rate of DNR-loaded NP group was slightly higher than that of DNR group, but there was no statistical difference between them ($P>0.05$; Figure 6).

Discussion

One hundred years ago, Ehrlich, the founder of chemotherapy, created the "magic bullets" theory. He conceived that the chemotherapy drug can selectively target tumor cells and avoid damage to normal cells. His postulate inspired generations of scientists to devise powerful molecular cancer target therapeutics.[13] Nowadays, tumor targeting therapies have become the mainstream of cancer therapy,[14] in which an appropriate drug carrier system is the key to improve the therapeutic effect of antitumor drugs. As a result, the nano drug carrier technology has been developed.[15–17]

It is found that PLGA NPs, which received approval for human use, granted by the US Food and Drug Administration can improve the solubility and stability of antitumor drug, easily permeate the capillary, prolong the cycle time of drugs in the body, and improve the pharmacokinetic properties of drugs.[18,19] A previous study has shown that the PLGA-based NP carrier system can enhance drug penetration and improve antitumor effect in vivo.[20] Kalaria et al[21] also found that a PLGA adriamycin NP drug can improve the bioavailability of chemotherapy drugs and reduce systemic toxicity of adriamycin. Notably, the surface modification of PLGA NPs can

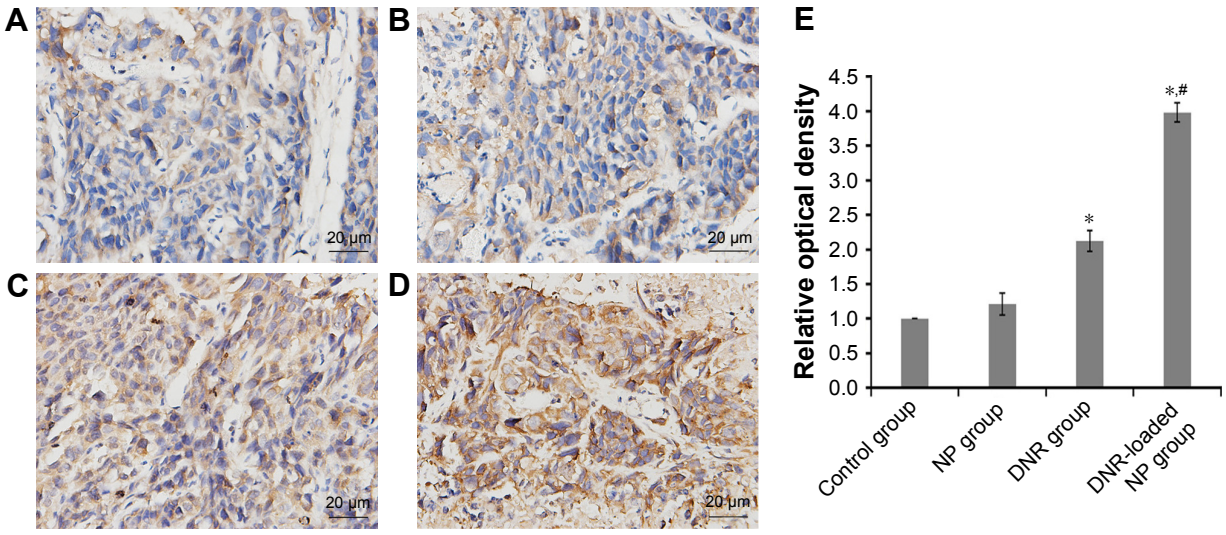

Figure 4 Representative images (**A**–**D**) and mean optical densities of Caspase 3 (**E**) by immunohistochemical staining (×400) and Image Pro Plus. (**A**) Control group; (**B**) NP group; (**C**) DNR group; and (**D**) DNR-loaded NP group. *$P<0.05$ when compared with the control group, #$P<0.05$ when compared with the DNR group.
Abbreviations: DNR, daunorubicin; NP, nanoparticle.

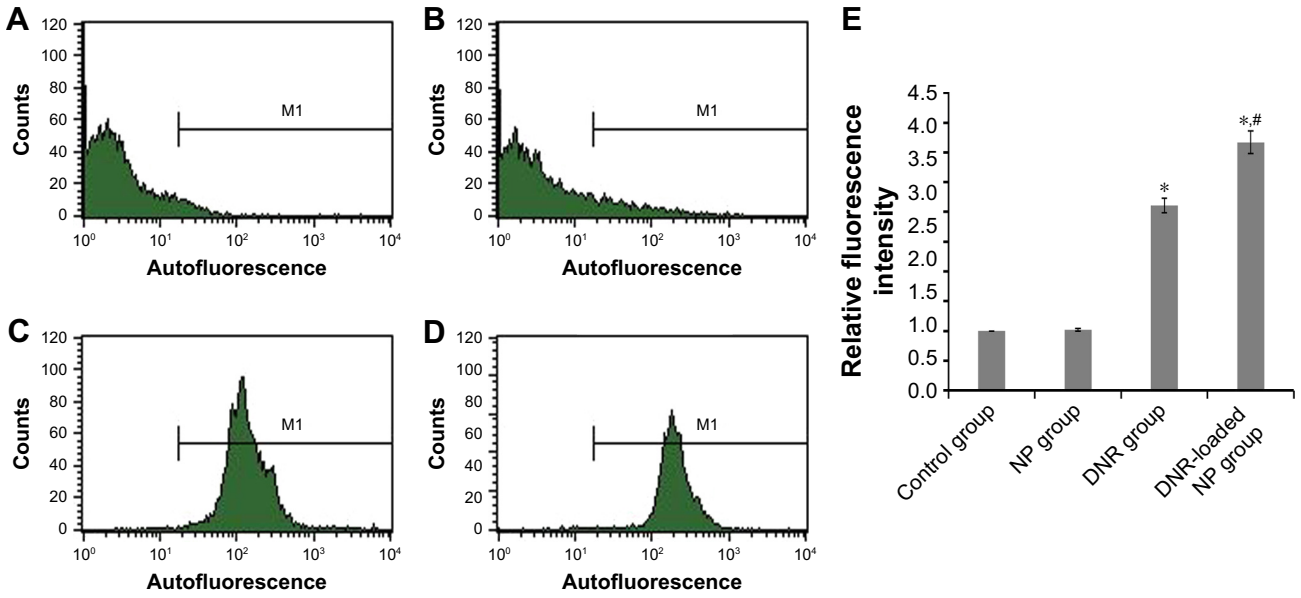

Figure 5 Intracellular accumulation of DNR (**A**–**D**) and relative fluorescence intensity (**E**) in primary acute leukemia cells by FCM assay. (**A**) Control group; (**B**) NP group; (**C**) DNR group; and (**D**) DNR-loaded NP group. *$P<0.05$ when compared with the control group, #$P<0.05$ when compared with the DNR group.
Abbreviations: DNR, daunorubicin; NP, nanoparticle; FCM, flow cytometry.

also target drug delivery to the tumor cells and reduce drug adverse reactions to the normal cells.[22] In addition, PEG is widely used in the drug delivery field due to its long history of safety in humans. Coating the surface of NPs with PEG can prolong systemic circulation time and shield the surface from aggregation, opsonization, and phagocytosis.[23] Therefore, PEG coatings on NPs are commonly used for improving the efficiency of drug delivery to target cells.[24] Recently, it has been demonstrated that PLL seems to be the backbone of drug delivery carrier based on its water-soluble, hydro-degradable, biodegradable, and biocompatible properties.[25] Using lung cancer A549 cells, Tahara et al reported that PLL-modified PLGA nanospheres were taken up by cells in remarkably higher amounts than unmodified nanospheres.[26]

In this experiment, we used biodegradable polymeric PLGA-PLL-PEG-Tf NPs as the DDS to explore whether

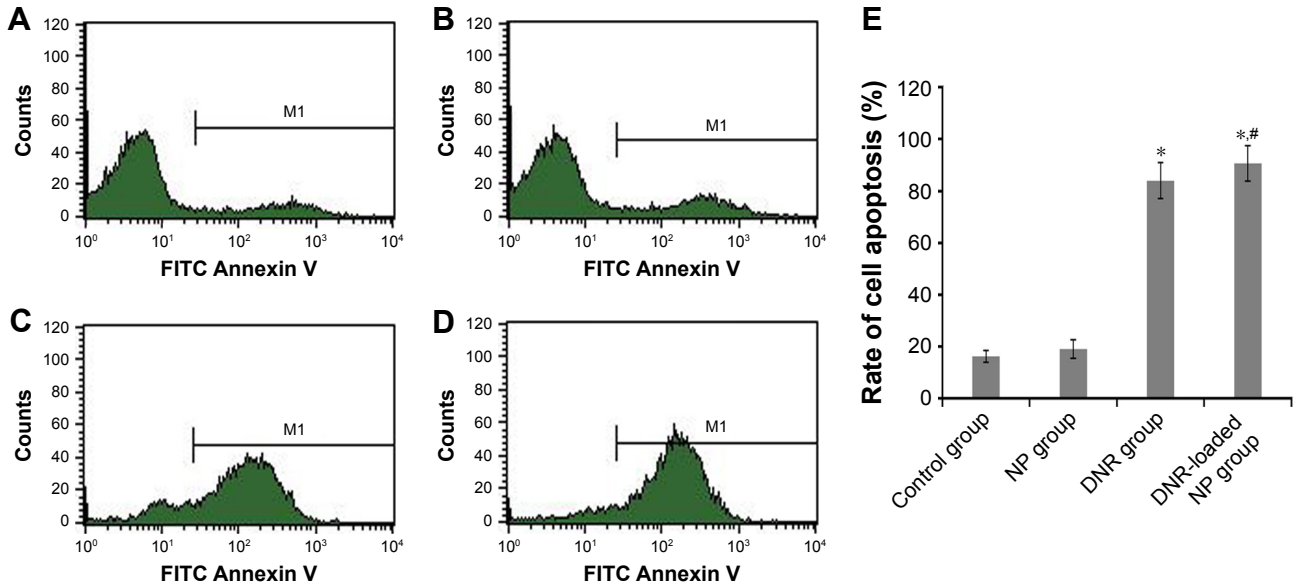

Figure 6 Representative images of cell apoptosis determined by flow cytometry (**A**–**D**) and apoptosis rate (**E**) in primary leukemia cells. (**A**) Control group; (**B**) NP group; (**C**) DNR group; and (**D**) DNR-loaded NP group. *$P<0.05$ when compared with control group; #$P>0.05$ when compared with DNR group.
Abbreviations: DNR, daunorubicin; NP, nanoparticles.

the NP delivery can improve the efficacy of cancer therapy. DNR-loaded NPs observed under SEM were spherical or nearly spherical, the diameter of which was about 180 nm.[12] In addition, our previous study reported the mean size and zeta-potential of DNR-loaded NPs were 176.4±11.0 nm and −19.24±0.12 mV, respectively.[11] Recently, Liu et al have been reported that the encapsulation efficiency and moderate drug loading of DNR-loaded NPs were 70.23%±1.91% and 3.63%±0.15% for DNR, respectively.[12] Thus, PLGA-PLL-PEG formulation is a potential DDS for hydrophilic and hydrophobic drugs, and Tf modification may increase its targeting properties.[12] All these results show that DNR-PLGA-PLL-PEG-Tf NPs are suitable for drug delivery.[27]

NP DDS showed prolonged circulation times in vivo and accumulation at particular sites due to the balance between diffusion mechanisms and vascular hemodynamic forces.[28] NPs were transferred from the surrounding vessels into the tumor through large gaps between adjacent endothelial cells in tumor blood vessels due to the inherent leakiness of tumor microvasculature. It is recognized that passive drug targeting is widely exploited in chemotherapy because NPs can be made to accumulate in tumor tissues based on the enhanced permeation and retention effect.[29,30] However, passive targeting strategies have shown several limitations, thus active targeting NP DDS that can maximize the tumor drug accumulation in the tumor tissue has been investigated.[31,32] A previous study has demonstrated that the surface modification of NPs can improve the effect of active targeting and reduce drug adverse reactions to the normal cells.[33] Increasing evidence from multiple studies has shown that Tf, TfR, and their biological significance have been widely characterized.[34] Sinha et al reported that an upregulation of TfR level was detected in tumor cells compared to normal cells,[10] which may be related to the increased expression of TfR. Thereby, chemotherapy drugs connected with use of Tf as an active targeting strategy were designed to enhance therapeutic cellular concentrations and increase drug efficacy through TfR and Tf-mediated endocytic mechanisms.

In this study, no obvious toxicity was observed in animals during treatment, and the intracellular distribution of DNR in K562 cells was visible in the DNR group and DNR-loaded NP group detected by fluorescence microscopy,[35] notably the intracellular drug concentration of DNR-loaded NP group was higher than that of DNR group. Furthermore, in vivo, tumor inhibitory rate was significantly higher in the DNR-loaded NP group than that in the DNR group.[11] These results infer that PLGA-PLL-PEG-Tf NPs may be a promising strategy to directly deliver antitumor drugs into tumor tissues and increase antitumor activities via passive and active targeting strategies.

Apoptosis is highly regulated in eukaryotic cells, in which Caspase family of proteins play a key role in the initiation and execution of apoptosis, especially Caspase 3 is an executioner of apoptosis in a variety of normal tissues and tumors. However, many cancer cells evade cell death program due to mutations in Caspases.[36] In our study, the total levels of Caspase 3 in both DNR group and DNR-loaded NP group were upregulated compared with control group. Notably, the total level of Caspase 3 in DNR-loaded NP group was obviously higher than that in DNR group. These data indicate that targeted this NP DDS substantially enhances the antitumor activity of traditional chemotherapeutic agents by inducing apoptosis in a Caspase-dependent manner.

Acute myeloid leukemia is a malignant disease of the hematopoietic system characterized by clonal accumulation and expansion of immature myeloid cells. As we know, primary leukemia cells have the characteristics of high homology with the cells in vivo, usually used in experimental research in leukemia study.[37] In our study, primary leukemia cells from acute myeloid leukemia were incubated with saline, NPs, DNR, and DNR-loaded NPs. Higher intracellular concentration of DNR was detected in both DNR and DNR-loaded NP groups compared with the control group. In addition, the intracellular distribution of DNR was significantly stronger in DNR-loaded NP group than that in DNR group, suggesting that the NPs enhance the accumulation of DNR in primary leukemia cells. Besides that, apoptosis rate in primary cells was also measured after incubation for 48 hours, and the results of FCM demonstrated that the apoptosis rate of DNR-loaded NP group was slightly higher than that of DNR group; however, there was no significant difference between them. In vivo, the inhibitory rate in xenograft tumors in the DNR-loaded NP group was significantly higher compared with DNR group after treatment for 18 days. Furthermore, the levels of Caspase 3 in the xenograft tumor tissues of DNR-loaded NP group were upregulated compared with DNR group. Notably, in our previous study, we found that the drug could be delivered to the targeted tumor cells and released slowly from the delivery system with the NP skeleton degradation.[38] Thus, we infer that DNR-loaded NPs provide a targeted anti-tumor effect by inducing remarkable cell apoptosis and inhibiting the proliferation of leukemia cells via sustained release drugs.

Conclusion

In summary, PLGA-PLL-PEG-Tf NP, as a passive and active targeting strategy, can accumulate the drugs at the

intracellular target region and release drugs smoothly from the nano DDS to kill tumor cells, avoiding systematic toxicity. However, further research in vivo should be conducted to demonstrate its bright future in the treatment of patients with hematologic malignancies.

Acknowledgments

This work was supported by the National Natural Science Foundation of China (Grant No 81600161), the Natural Science Foundation of Jiangsu Province (Grant No BK 20180372), and Key Discipline of Jiangsu Province (ZDXKB2016020).

Disclosure

The authors report no conflicts of interest in this work.

References

1. Tortorella S, Karagiannis TC. Transferrin receptor-mediated endocytosis: a useful target for cancer therapy. *J Membr Biol*. 2014;247:291–307. doi:10.1007/s00232-014-9637-0
2. Daniels TR, Delgado T, Rodriguez JA, Helguera G, Penichet ML. The transferrin receptor part I: biology and targeting with cytotoxic antibodies for the treatment of cancer. *Clin Immunol*. 2006;121:144–158. doi:10.1016/j.clim.2006.06.010
3. Kazan HH, Urfali-Mamatoglu C, Gunduz U. Iron metabolism and drug resistance in cancer. *Biometals*. 2017;30(5):629–641. doi:10.1007/s10534-017-0037-7
4. Sakurai K, Sohda T, Ueda S, et al. Immunohistochemical demonstration of transferrin receptor 1 and 2 in human hepatocellular carcinoma tissue. *Hepatogastroenterology*. 2014;61(130):426–430.
5. Yang DC, Wang F, Elliott RL, Head JF. Expression of transferrin receptor and ferritin H-chain mRNA are associated with clinical and histopathological prognostic indicators in breast cancer. *Anticancer Res*. 2001;21:541–549.
6. Das Gupta A, Shah VI. Correlation of transferrin receptor expression with histologic grade and immunophenotype in chronic lymphocytic leukemia and non-Hodgkin's lymphoma. *Hematol Pathol*. 1990;4:37–41.
7. Gomme PT, McCann KB, Bertolini J. Transferrin: structure, function and potential therapeutic actions. *Drug Discov Today*. 2005;10:267–273. doi:10.1016/S1359-6446(04)03333-1
8. Shinohara H, Fan D, Ozawa S, et al. Site-specific expression of transferrin receptor by human colon cancer cells directly correlates with eradication by antitransferrin recombinant immunotoxin. *Int J Oncol*. 2000;17:643–651.
9. Parveen S, Misra R, Sahoo SK. Nanoparticles: a boon to drug delivery, therapeutics, diagnostics and imaging. *Nanomedicine*. 2012;8:147–166. doi:10.1016/j.nano.2011.05.016
10. Sinha R, Kim GJ, Nie S, Shin DM. Nanotechnology in cancer therapeutics: bioconjugated nanoparticles for drug delivery. *Mol Cancer Ther*. 2006;5:1909–1917. doi:10.1158/1535-7163.MCT-06-0141
11. Bao W, Liu R, Wang Y, et al. PLGA-PLL-PEG-Tf-based targeted nanoparticles drug delivery system enhance antitumor efficacy via intrinsic apoptosis pathway. *Int J Nanomedicine*. 2015;10:557–566. doi:10.2147/IJN.S75090
12. Liu R, Wang Y, Li X, et al. Synthesis and characterization of tumor-targeted copolymer nanocarrier modified by transferrin. *Drug Des Devel Ther*. 2015;9:2705–2719. doi:10.2147/DDDT.S80948
13. Strebhardt K, Ullrich A. Paul Ehrlich's magic bullet concept: 100 years of progress. *Nat Rev Cancer*. 2008;8:473–480. doi:10.1038/nrc2394
14. Collins I, Workman P. New approaches to molecular cancer therapeutics. *Nat Chem Biol*. 2006;2:689–700. doi:10.1038/nchembio840
15. Moghadam NH, Salehzadeh S, Rakhtshah J, et al. Improving antiproliferative effect of the nevirapine on Hela cells by loading onto chitosan coated magnetic nanoparticles as a fully biocompatible nano drug carrier. *Int J Biol Macromol*. 2018;118:1220–1228. doi:10.1016/j.ijbiomac.2018.06.144
16. Kim BY, Rutka JT, Chan WC. Nanomedicine. *N Engl J Med*. 2010;363:2434–2443. doi:10.1056/NEJMra0912273
17. Doane TL, Burda C. The unique role of nanoparticles in nanomedicine: imaging, drug delivery and therapy. *Chem Soc Rev*. 2012;41:2885–2911. doi:10.1039/c2cs15260f
18. Soppimath KS, Aminabhavi TM, Kulkarni AR, et al. Biodegradable polymeric nanoparticles as drug delivery devices. *J Control Release*. 2001;70:1–20.
19. Colzani B, Pandolfi L, Hoti A, et al. Investigation of antitumor activities of trastuzumab delivered by PLGA nanoparticles. *Int J Nanomedicine*. 2018;14(13):957–973. doi:10.2147/IJN.S152742
20. Ranganath SH, Fu Y, Arifin DY, et al. The use of submicron/nanoscale PLGA implants to deliver paclitaxel with enhanced pharmacokinetics and therapeutic efficacy in intracranial glioblastoma in mice. *Biomaterials*. 2010;31:5199–5207. doi:10.1016/j.biomaterials.2010.03.002
21. Kalaria DR, Sharma G, Beniwal V, Ravi Kumar MNV. Design of biodegradable nanoparticles for oral delivery of doxorubicin: in vivo pharmacokinetics and toxicity studies in rats. *Pharm Res*. 2009;26:492–501. doi:10.1007/s11095-008-9763-4
22. Nobs L, Buchegger F, Gurny R, Allémann E. Poly(lactic acid) nanoparticles labeled with biologically active Neutravidin for active targeting. *Eur J Pharm Biopharm*. 2004;58:483–490. doi:10.1016/j.ejpb.2004.04.006
23. Grossen P, Witzigmann D, Sieber S, Huwyler J. PEG-PCL-based nanomedicines: a biodegradable drug delivery system and its application. *Control Release*. 2017;260:46–60. doi:10.1016/j.jconrel.2017.05.028
24. Suk JS, Xu Q, Kim N, et al. PEGylation as a strategy for improving nanoparticle-based drug and gene delivery. *Adv Drug Deliv Rev*. 2016;99(Pt A):28–51. doi:10.1016/j.addr.2015.09.012
25. Umano M, Uechi K, Uriuda T, et al. Tumor accumulation of ε-polylysines-based polyamines conjugated with boron clusters. *Appl Radiat Isot*. 2011;69(12):1765–1767. doi:10.1016/j.apradiso.2011.02.048
26. Tahara K, Furukawa S, Yamamoto H, Kawashima Y. Hybrid-modified poly(D,L-lactide-co-glycolide) nanospheres for a novel cellular drug delivery system. *Int Pharm*. 2010;392(1–2):311–313. doi:10.1016/j.ijpharm.2010.03.042
27. Petros RA, DeSimone JM. Strategies in the design of nanoparticles for therapeutic applications. *Nat Rev Drug Discov*. 2010;9:615–627. doi:10.1038/nrd2591
28. Sanna V, Pala N, Sechi M. Targeted therapy using nanotechnology: focus on cancer. *Int J Nanomedicine*. 2014;9:467–483. doi:10.2147/IJN.S36654
29. Maeda H, Wu J, Sawa T, Matsumura Y, Hori K. Tumor vascular permeability and the EPR effect in macromolecular therapeutics: a review. *J Control Release*. 2000;65:271–284.
30. Huang Y, Fan C-Q, Dong H, Wang S-M, Yang X-C, Yang S-M. Current applications and future prospects of nanomaterials in tumor therapy. *Int J Nanomedicine*. 2017;12:1815–1825. doi:10.2147/IJN.S127349
31. Lammers T, Kiessling F, Hennink WE, Storm G. Drug targeting to tumors: principles, pitfalls and (pre-) clinical progress. *J Control Release*. 2012;161:175–187. doi:10.1016/j.jconrel.2011.09.063
32. Davis ME, Chen ZG, Shin DM. Nanoparticle therapeutics: an emerging treatment modality for cancer. *Nat Rev Drug Discov*. 2008;7:771–782. doi:10.1038/nrd2614
33. Byrne JD, Betancourt T, Brannon-Peppas L. Active targeting schemes for nanoparticle systems in cancer therapeutics. *Adv Drug Deliv Rev*. 2008;60:1615–1626. doi:10.1016/j.addr.2008.08.005
34. Choi J-S, Park J-S. Development of docetaxel nanocrystals surface modified with transferrin for tumor targeting. *Drug Des Devel Ther*. 2016;11:17–26. doi:10.2147/DDDT.S122984

35. Gong Y-P, Liu T, Jia Y-Q, Qin L, Deng C-Q, Yang R-YO. Comparison of Pgp- and MRP-mediated multidrug resistance in leukemia cell lines. *Int J Hematol*. 2002;75(2):154–160.
36. Brentnall M, Rodriguez-Menocal L, De Guevara RL, et al. Caspase-9, caspase-3 and caspase-7 have distinct roles during intrinsic apoptosis. *BMC Cell Biol*. 2013;14:32. doi:10.1186/1471-2121-14-50
37. Kino-Oka M, Taya M. Recent developments in processing systems for cell and tissue cultures toward therapeutic application. *J Biosci Bioeng*. 2009;108:267–276. doi:10.1016/j.jbiosc.2009.04.007
38. Cheng J, Wang J, Chen B, et al. A promising strategy for overcoming MDR in tumor by magnetic iron oxide nanoparticles co-loaded with daunorubicin and 5-bromotetrandrin. *Int J Nanomedicine*. 2011;6:2123–2131. doi:10.2147/IJN.S24309